PERGAMON

International Journal of Solids and Structures 38 (2001) 2549–2571

INTERNATIONAL JOURNAL OF SOLIDS and STRUCTURES

www.elsevier.com/locate/ijsolstr

Multiple scattering of plane elastic waves in a fiber-reinforced composite medium with graded interfacial layers

Hirotaka Sato, Yasuhide Shindo *

Department of Materials Processing, Graduate School of Engineering, Tohoku University, Aoba-yama 02, Sendai 980-8579, Japan

Received 11 August 1999; in revised form 3 April 2000

Abstract

In this study, we consider the multiple scattering of time-harmonic elastic waves in a metal matrix composite containing randomly distributed parallel fibers with graded interfacial layers. In-plane compressional and shear waves are considered. We assume same-size circular fibers of identical properties and same-thickness interface layers with nonhomogeneous elastic properties. The method of solution consists of first solving the scattering problem by a large number N of arbitrarily distributed fibers in an infinite matrix, the resulting equations are then averaged by considering the positions of the fibers to be random with a statistically uniform distribution, and these averaged equations are solved by using Lax's quasicrystalline approximation. Numerical calculations for a SiC-fiber-reinforced Al composite are carried out for a moderately wide range of frequencies and the effect of interface properties on the phase velocities, attenuations of coherent plane waves and the effective elastic moduli are shown graphically.

Keywords: Elasticity; Wave; Scattering; Composite materials; Fiber reinforced; Inclusions; Interface; Functionally graded

1. Introduction

The wave propagation through a composite medium with a random distribution of inclusions, with interface layers, has been a subject of recent practical interest (Shindo et al., 1995; Shindo and Niwa, 1996; Nozaki and Shindo, 1998). Recently, Shindo et al. (1998) analyzed the multiple scattering of anti-plane shear waves in a metal matrix composite reinforced by fibers with interface layers.

The purpose of this study is to analyze the effects of graded interface layers and multiple scattering by a distribution of fibers on the wave propagation of time-harmonic plane elastic waves in a fiber-reinforced metal matrix composite. The same-size circular fibers of identical properties with same-thickness nonhomogeneous interface layers are assumed to be parallel to each other and randomly distributed with a statistically uniform distribution. In-plane problem is studied, and both the direction of propagation and the particle motion of the wave are at right angles to the fibers. The problem of the scattering of plane

* Corresponding author. Tel.: +81-22-217-7341; fax: +81-22-217-7341.
E-mail address: shindo@msws.material.tohoku.ac.jp (Y. Shindo).

0020-7683/01/$ - see front matter
PII: S0020-7683(00)00170-0

compressional (P) and shear (SV) waves by a large number N of circular fibers, arbitrarily distributed in an infinite matrix, is analyzed and the resulting equations are then averaged, considering the positions of the fibers to be random (Bose and Mal, 1974). The averaged equations are solved by using Lax's quasicrystalline approximation to yield the propagation characteristics of the average waves (Lax, 1952). The particular case when the pair correlation function has an exponential form is examined in detail. The complex wave numbers giving the phase velocities and the attenuations of coherent plane elastic waves, and the effective elastic moduli for a SiC-fiber-reinforced Al composite are obtained numerically and shown in graphs for various interface properties at designated frequencies. The method of solution is a generalization of the previous one (Shindo et al., 1998).

2. Statement of the problem and scattering of in-plane compressional and shear waves by N fibers

We suppose the identical circular fibers of radius a_0 to be located within a large region S in an infinite matrix. Let λ, μ, ρ, v be the Lamé constants, the mass density, the Poisson's ratio of the matrix, and λ_0, μ_0, ρ_0, v_0 those of the fibers. Let the fiber be separated from the matrix by a thick layer of uniform thickness h with variable material properties. The geometry is depicted in Fig. 1, where (x, y, z) is the Cartesian coordinate system with origin at o and (r, θ, z) is the corresponding cylindrical coordinate system. The layer is composed of n cylindrical shells of homogeneous isotropic materials, and the material properties within

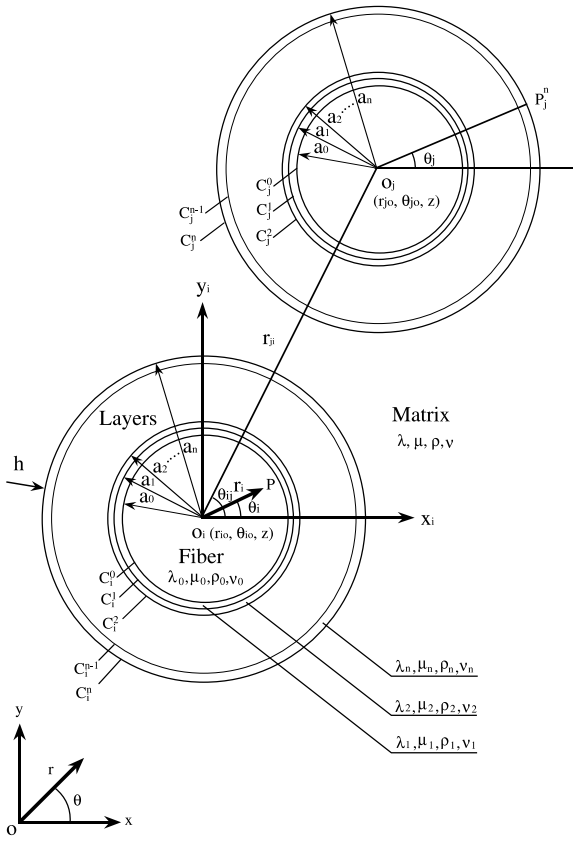

Fig. 1. Circular fibers with interface layers and coordinate systems.

each shell of inner radius a_{l-1}, outer radius a_l $(l = 1, 2, \ldots, n)$ and uniform thickness $h_l = a_l - a_{l-1}$ are λ_l, μ_l, ρ_l, v_l. Labeling the fibers by suffixes $i = 1, 2, \ldots, N$ and taking suitable coordinate axes in a transverse plane, let the boundaries of the ith circular fiber and the shells be denoted by C_i^l $(l = 0, 1, 2, \ldots, n)$ and the Cartesian and cylindrical coordinates of those center o_i $(r_{io},\ \theta_{io},\ z)$ be $(x_i,\ y_i,\ z)$ and $(r_i,\ \theta_i,\ z)$, respectively.

The displacement components in r and θ directions are u_r and u_θ while the component u_z is absent because the problem is plane strain. For the same reason, derivatives with respect to z are zero. Under these conditions, the displacement components may be expressed in terms of two wave potentials $\Phi(r, \theta, t)$ and $\Psi(r, \theta, t)$, where t is the time by the following relationships:

$$\begin{cases} u_r = \frac{\partial \Phi}{\partial r} + \frac{1}{r}\frac{\partial \Psi}{\partial \theta}, \\ u_\theta = \frac{1}{r}\frac{\partial \Phi}{\partial \theta} - \frac{\partial \Psi}{\partial r}, \\ u_z = 0, \end{cases} \tag{1}$$

where Φ and Ψ are wave potentials. Substituting Eq. (1) into Hooke's law for a homogeneous and isotropic elastic solid yields the following expressions for the stress components σ_{rr}, $\sigma_{\theta\theta}$ and $\sigma_{r\theta}$:

$$\begin{cases} \sigma_{rr} = \lambda\left(\frac{\partial^2 \Phi}{\partial r^2} + \frac{1}{r}\frac{\partial \Phi}{\partial r} + \frac{1}{r^2}\frac{\partial^2 \Phi}{\partial \theta^2}\right) + 2\mu\left(\frac{\partial^2 \Phi}{\partial r^2} - \frac{1}{r^2}\frac{\partial \Psi}{\partial \theta} + \frac{1}{r}\frac{\partial^2 \Psi}{\partial r \partial \theta}\right), \\ \sigma_{\theta\theta} = \lambda\left(\frac{\partial^2 \Phi}{\partial r^2} + \frac{1}{r}\frac{\partial \Phi}{\partial r} + \frac{1}{r^2}\frac{\partial^2 \Phi}{\partial \theta^2}\right) + 2\mu\left(\frac{1}{r^2}\frac{\partial^2 \Phi}{\partial \theta^2} + \frac{1}{r}\frac{\partial \Phi}{\partial r} - \frac{1}{r}\frac{\partial^2 \Psi}{\partial r \partial \theta} + \frac{1}{r^2}\frac{\partial \Psi}{\partial \theta}\right), \\ \sigma_{r\theta} = \mu\left(\frac{2}{r}\frac{\partial^2 \Phi}{\partial r \partial \theta} - \frac{2}{r^2}\frac{\partial \Phi}{\partial \theta} + \frac{1}{r^2}\frac{\partial^2 \Psi}{\partial \theta^2} - \frac{\partial^2 \Psi}{\partial r^2} + \frac{1}{r}\frac{\partial \Psi}{\partial r}\right). \end{cases} \tag{2}$$

By making use of Eq. (2), the equations of motion of elasticity yield the following equations governing the potentials Φ and Ψ:

$$\nabla^2 \Phi = \frac{1}{c_{\mathrm{p}}^2}\frac{\partial^2 \Phi}{\partial t^2}, \qquad \nabla^2 \Psi = \frac{1}{c_{\mathrm{sv}}^2}\frac{\partial^2 \Psi}{\partial t^2}, \tag{3}$$

where $\nabla^2 = \partial^2/\partial r^2 + (1/r)\partial/\partial r + (1/r^2)\partial^2/\partial\theta^2$ is the Laplacian operator in variables r and θ, and c_{p}, c_{sv} are the compressional and shear wave speeds in the matrix,

$$c_{\mathrm{p}} = \left(\frac{\lambda + 2\mu}{\rho}\right)^{1/2}, \qquad c_{\mathrm{sv}} = \left(\frac{\mu}{\rho}\right)^{1/2}. \tag{4}$$

We consider P wave propagating in the positive x-direction or a plane shear SV wave polarized in the y-direction and propagating in the positive x-direction. Thus,

$$\begin{cases} \Phi^i = \Phi_0 \exp\{\mathrm{i}(k_{\mathrm{p}} x - \omega t)\}, \\ \Psi^i = \Psi_0 \exp\{\mathrm{i}(k_{\mathrm{sv}} x - \omega t)\}, \end{cases} \tag{5}$$

where a superscript i stands for the incident component, ω is the circular frequency of the wave and Φ_0, Ψ_0 are the amplitudes of the incident P and SV waves. k_{p} and k_{sv} are the wave numbers of the compressional and shear waves in the matrix,

$$k_{\mathrm{p}} = \frac{\omega}{c_{\mathrm{p}}}, \qquad k_{\mathrm{sv}} = \frac{\omega}{c_{\mathrm{sv}}}. \tag{6}$$

The wave potentials Φ^i and Ψ^i can be expanded as the summation of cylindrical functions as

$$\begin{cases} \Phi^i = \Phi_0 \exp(\mathrm{i}k_{\mathrm{p}} r_{io} \cos\theta_{io}) \sum_{m=-\infty}^{\infty} i^m J_m(k_{\mathrm{p}} r_i) \exp\{\mathrm{i}(m\theta_i - \omega t)\}, \\ \Psi^i = \Psi_0 \exp(\mathrm{i}k_{\mathrm{sv}} r_{io} \cos\theta_{io}) \sum_{m=-\infty}^{\infty} i^m J_m(k_{\mathrm{sv}} r_i) \exp\{\mathrm{i}(m\theta_i - \omega t)\}, \end{cases} \tag{7}$$

where $J_m(\ )$ is the mth order Bessel function of the first kind (Watson, 1966). In what follows, the time factor $\exp(-\mathrm{i}\omega t)$ will be omitted from all the field quantities.

The potential fields in the matrix, the lth layer of the ith circular fiber and the ith circular fiber may be expressed in the forms

$$\begin{cases} \Phi^s = \sum_{i=1}^{N} \Phi_i^s, \\ \Phi_i^s = \sum_{m=-\infty}^{\infty} A_{im} H_m(k_\mathrm{p} r_i) \exp(\mathrm{i}m\theta_i), \\ \Psi^s = \sum_{i=1}^{N} \Psi_i^s, \\ \Psi_i^s = \sum_{m=-\infty}^{\infty} B_{im} H_m(k_\mathrm{sv} r_i) \exp(\mathrm{i}m\theta_i), \end{cases} \tag{8}$$

$$\begin{cases} \Phi_i^l = \sum_{m=-\infty}^{\infty} [A_{im}^l H_m(k_\mathrm{p}^l r_i) + C_{im}^l J_m(k_\mathrm{p}^l r_i)] \exp(\mathrm{i}m\theta_i), \\ \Psi_i^l = \sum_{m=-\infty}^{\infty} [B_{im}^l H_m(k_\mathrm{sv}^l r_i) + D_{im}^l J_m(k_\mathrm{sv}^l r_i)] \exp(\mathrm{i}m\theta_i), \end{cases} \tag{9}$$

$$\begin{cases} \Phi_i^t = \sum_{m=-\infty}^{\infty} C_{im}^0 J_m(k_\mathrm{p}^0 r_i) \exp(\mathrm{i}m\theta_i), \\ \Psi_i^t = \sum_{m=-\infty}^{\infty} D_{im}^0 J_m(k_\mathrm{sv}^0 r_i) \exp(\mathrm{i}m\theta_i), \end{cases} \tag{10}$$

where superscripts s, t and l ($l = 1, 2, \ldots, n$) denote the scattered component within a matrix, the transmitted component within a circular fiber and the field quantity within an lth layer. A_{im}, B_{im}, A_{im}^l, B_{im}^l, C_{im}^l, D_{im}^l, C_{im}^0 and D_{im}^0 are the unknowns to be solved and $H_m(\ )$ is the mth order Hankel function of the first kind. The wave numbers k_p^l, k_sv^l ($l = 1, 2, \ldots, n$) in the lth layer and k_p^0, k_sv^0 in the circular fiber are given by

$$\begin{cases} k_\mathrm{p}^l = \frac{\omega}{c_\mathrm{p}^l}, \quad k_\mathrm{sv}^l = \frac{\omega}{c_\mathrm{sv}^l} \qquad (l = 1, 2, \ldots, n), \\ k_\mathrm{p}^0 = \frac{\omega}{c_\mathrm{p}^0}, \quad k_\mathrm{sv}^0 = \frac{\omega}{c_\mathrm{sv}^0}, \end{cases} \tag{11}$$

where the compressional and shear wave speeds c_p^l, c_sv^l in the lth layer and c_p^0, c_sv^0 in the circular fiber are

$$\begin{cases} c_\mathrm{p}^l = \left(\frac{\lambda_l + 2\mu_l}{\rho_l}\right)^{1/2}, \quad c_\mathrm{sv}^l = \left(\frac{\mu_l}{\rho_l}\right)^{1/2} \qquad (l = 1, 2, \ldots, n), \\ c_\mathrm{p}^0 = \left(\frac{\lambda_0 + 2\mu_0}{\rho_0}\right)^{1/2}, \quad c_\mathrm{sv}^0 = \left(\frac{\mu_0}{\rho_0}\right)^{1/2}. \end{cases} \tag{12}$$

The total scattered field (8) in the matrix is taken to be a superposition of the scattered fields of every fiber, where the latters can be expressed as the series representation of Hankel functions satisfying the outgoing conditions at infinity.

The boundary conditions on C_j^l ($l = 0, 1, 2, \ldots, n$) are

$$\begin{cases} u_{rj}^n = u_{rj}^s + u_{rj}^i, \quad \sigma_{rrj}^n = \sigma_{rrj}^s + \sigma_{rrj}^i \\ u_{\theta j}^n = u_{\theta j}^s + u_{\theta j}^i, \quad \sigma_{r\theta j}^n = \sigma_{r\theta j}^s + \sigma_{r\theta j}^i \end{cases} \qquad (r_j = a_n), \tag{13}$$

$$\begin{cases} u_{rj}^l = u_{rj}^{l+1}, \quad \sigma_{rrj}^l = \sigma_{rrj}^{l+1} \\ u_{\theta j}^l = u_{\theta j}^{l+1}, \quad \sigma_{r\theta j}^l = \sigma_{r\theta j}^{l+1} \end{cases} \qquad (r_j = a_l,\ l = 1, 2, \ldots, n-1), \tag{14}$$

$$\begin{cases} u^t_{rj} = u^1_{rj}, \quad \sigma^t_{rrj} = \sigma^1_{rrj} \\ u^t_{\theta j} = u^1_{\theta j}, \quad \sigma^t_{r\theta j} = \sigma^1_{r\theta j} \end{cases} \qquad (r_j = a_0). \tag{15}$$

Then, using the condition of continuity of displacement at $P^n_j(a_n, \theta_j, z)$ on C^n_j, multiplying by $\exp(-\mathrm{i}v\theta_j)$ and integrating from 0 to 2π, we have

$$\begin{cases} A^n_{jv}\frac{\partial}{\partial a_n}H_v(k^n_{\mathrm{p}}a_n) + \frac{\mathrm{i}v}{a_n}B^n_{jv}H_v(k^n_{\mathrm{sv}}a_n) + C^n_{jv}\frac{\partial}{\partial a_n}J_v(k^n_{\mathrm{p}}a_n) + \frac{\mathrm{i}v}{a_n}D^n_{jv}J_v(k^n_{\mathrm{sv}}a_n) \\ \quad = i^v\left\{\Phi_0\exp(\mathrm{i}k_{\mathrm{p}}r_{jo}\cos\theta_{jo})\frac{\partial}{\partial a_n}J_v(k_{\mathrm{p}}a_n) + \frac{\mathrm{i}v}{a_n}\Psi_0\exp(\mathrm{i}k_{\mathrm{sv}}r_{jo}\cos\theta_{jo})J_v(k_{\mathrm{sv}}a_n)\right\} \\ \qquad +\sum_{i=1}^{N}\sum_{m=-\infty}^{\infty}\left(A_{im}\frac{\partial}{\partial a_n}L_{ijmv} + \frac{\mathrm{i}v}{a_n}B_{im}K_{ijmv}\right), \\ \frac{\mathrm{i}v}{a_n}A^n_{jv}H_v(k^n_{\mathrm{p}}a_n) - B^n_{jv}\frac{\partial}{\partial a_n}H_v(k^n_{\mathrm{sv}}a_n) + \frac{\mathrm{i}v}{a_n}C^n_{jv}J_v(k^n_{\mathrm{p}}a_n) - D^n_{jv}\frac{\partial}{\partial a_n}J_v(k^n_{\mathrm{sv}}a_n) \\ \quad = i^v\left\{\frac{\mathrm{i}v}{a_n}\Phi_0\exp(\mathrm{i}k_{\mathrm{p}}r_{jo}\cos\theta_{jo})J_v(k_{\mathrm{p}}a_n) - \Psi_0\exp(\mathrm{i}k_{\mathrm{sv}}r_{jo}\cos\theta_{jo})\frac{\partial}{\partial a_n}J_v(k_{\mathrm{sv}}a_n)\right\} \\ \qquad +\sum_{i=1}^{N}\sum_{m=-\infty}^{\infty}\left(\frac{\mathrm{i}v}{a_n}A_{im}L_{ijmv} - B_{im}\frac{\partial}{\partial a_n}K_{ijmv}\right), \end{cases} \tag{16}$$

where

$$\begin{cases} L_{ijmv} &= \frac{1}{2\pi}\int_0^{2\pi}\{H_m(k_{\mathrm{p}}r_i)\exp(\mathrm{i}m\theta_i)\}_{P^n_j}\exp(-\mathrm{i}v\theta_j)\,\mathrm{d}\theta_j \quad (i \neq j), \\ &= H_m(k_{\mathrm{p}}a_n)\delta_{mv} \quad (i = j), \\ K_{ijmv} &= \frac{1}{2\pi}\int_0^{2\pi}\{H_m(k_{\mathrm{sv}}r_i)\exp(\mathrm{i}m\theta_i)\}_{P^n_j}\exp(-\mathrm{i}v\theta_j)\,\mathrm{d}\theta_j \quad (i \neq j), \\ &= H_m(k_{\mathrm{sv}}a_n)\delta_{mv} \quad (i = j). \end{cases} \tag{17}$$

δ_{mv} is the Kronecker delta. Using the addition theorem of Hankel functions (Bose and Mal, 1973), we get

$$\begin{cases} L_{ijmv} &= \frac{1}{2\pi}\int_0^{2\pi}\left[\exp(\mathrm{i}m\theta_{ji})(-1)^m\sum_{s=-\infty}^{\infty}(-1)^s J_s(k_{\mathrm{p}}a_n)\,H_{s-m}(k_{\mathrm{p}}r_{ji})\exp\{\mathrm{i}s(\theta_j-\theta_{ji})\}\right] \\ &\quad \times\exp(-\mathrm{i}v\theta_j)\,\mathrm{d}\theta_j = J_v(k_{\mathrm{p}}a_n)H_{m-v}(k_{\mathrm{p}}r_{ji})\exp\{\mathrm{i}(m-v)\theta_{ji}\} \quad (i \neq j), \\ K_{ijmv} &= \frac{1}{2\pi}\int_0^{2\pi}\left[\exp(\mathrm{i}m\theta_{ji})(-1)^m\sum_{s=-\infty}^{\infty}(-1)^s J_s(k_{\mathrm{sv}}a_n)\,H_{s-m}(k_{\mathrm{sv}}r_{ji})\exp\{\mathrm{i}s(\theta_j-\theta_{ji})\}\right] \\ &\quad \times\exp(-iv\theta_j)\,\mathrm{d}\theta_j = J_v(k_{\mathrm{sv}}a_n)H_{m-v}(k_{\mathrm{sv}}r_{ji})\exp\{\mathrm{i}(m-v)\theta_{ji}\} \quad (i \neq j), \end{cases} \tag{18}$$

where (r_{ji}, θ_{ji}) are the polar coordinates of o_j referred to o_i as origin. Thus, Eq. (16) becomes

$$\mathbf{M}_v(k^n_{\mathrm{p}}a_n, k^n_{\mathrm{sv}}a_n)\begin{Bmatrix} A^n_{jv} \\ B^n_{jv} \end{Bmatrix} + \mathbf{K}_v(k^n_{\mathrm{p}}a_n, k^n_{\mathrm{sv}}a_n)\begin{Bmatrix} C^n_{jv} \\ D^n_{jv} \end{Bmatrix} = \mathbf{M}_v(k_{\mathrm{p}}a_n, k_{\mathrm{sv}}a_n)\begin{Bmatrix} A_{jv} \\ B_{jv} \end{Bmatrix} + \mathbf{K}_v(k_{\mathrm{p}}a_n, k_{\mathrm{sv}}a_n)\begin{Bmatrix} \Phi^j_v \\ \Psi^j_v \end{Bmatrix}, \tag{19}$$

where

$$\mathbf{M}_v(k^n_{\mathrm{p}}a_n, k^n_{\mathrm{sv}}a_n) = \begin{bmatrix} M^v_{11}(k^n_{\mathrm{p}}a_n) & M^v_{12}(k^n_{\mathrm{sv}}a_n) \\ M^v_{21}(k^n_{\mathrm{p}}a_n) & M^v_{22}(k^n_{\mathrm{sv}}a_n) \end{bmatrix}, \tag{20}$$

$$\begin{cases} M^v_{11}(k^n_{\mathrm{p}}a_n) = vH_v(k^n_{\mathrm{p}}a_n) - k^n_{\mathrm{p}}a_nH_{v+1}(k^n_{\mathrm{p}}a_n), \\ M^v_{12}(k^n_{\mathrm{sv}}a_n) = \mathrm{i}vH_v(k^n_{\mathrm{sv}}a_n), \\ M^v_{21}(k^n_{\mathrm{p}}a_n) = \mathrm{i}vH_v(k^n_{\mathrm{p}}a_n), \\ M^v_{22}(k^n_{\mathrm{sv}}a_n) = -\{vH_v(k^n_{\mathrm{sv}}a_n) - k^n_{\mathrm{sv}}a_nH_{v+1}(k^n_{\mathrm{sv}}a_n)\}, \end{cases} \tag{21}$$

and a similar expression for $\mathbf{K}_v(k^n_{\mathrm{p}}a_n, k^n_{\mathrm{sv}}a_n)$ with the vth order Hankel function of the first kind $H_v(\ )$ replaced by the vth order Bessel function of the first kind $J_v(\ )$ in Eqs. (20) and (21) is

$$\begin{cases} \Phi_v^j = i^v \Phi_0 \exp(\mathrm{i}k_\mathrm{p} r_{jo} \cos\theta_{jo}) + \sum_{i=1}^{N}{}' \sum_{m=-\infty}^{\infty} A_{i,m+v} H_m(k_\mathrm{p} r_{ji}) \exp(\mathrm{i}m\theta_{ji}), \\ \Psi_v^j = i^v \Psi_0 \exp(\mathrm{i}k_\mathrm{sv} r_{jo} \cos\theta_{jo}) + \sum_{i=1}^{N}{}' \sum_{m=-\infty}^{\infty} B_{i,m+v} H_m(k_\mathrm{sv} r_{ji}) \exp(\mathrm{i}m\theta_{ji}). \end{cases} \tag{22}$$

In Eq. (22), $\sum'$ denotes the sum over all circular fibers except the jth. Evidently, Φ_v^j and Ψ_v^j are related to the field at o_j if the jth fiber is assumed to be absent. The conditions of continuity of displacement at $P_j^l(a_l,\ \theta_j,\ z)$ on C_j^l $(l = 1, 2, \ldots, n-1)$ and $P_j^0(a_0,\ \theta_j,\ z)$ on C_j^0 give

$$\mathbf{M}_v(k_\mathrm{p}^l a_l, k_\mathrm{sv}^l a_l) \begin{Bmatrix} A_{jv}^l \\ B_{jv}^l \end{Bmatrix} + \mathbf{K}_v(k_\mathrm{p}^l a_l, k_\mathrm{sv}^l a_l) \begin{Bmatrix} C_{jv}^l \\ D_{jv}^l \end{Bmatrix} = \mathbf{M}_v(k_\mathrm{p}^{l+1} a_l, k_\mathrm{sv}^{l+1} a_l) \begin{Bmatrix} A_{jv}^{l+1} \\ B_{jv}^{l+1} \end{Bmatrix} + \mathbf{K}_v(k_\mathrm{p}^{l+1} a_l, k_\mathrm{sv}^{l+1} a_l) \begin{Bmatrix} C_{jv}^{l+1} \\ D_{jv}^{l+1} \end{Bmatrix}, \tag{23}$$

$$\mathbf{K}_v(k_\mathrm{p}^0 a_0, k_\mathrm{sv}^0 a_0) \begin{Bmatrix} C_{jv}^0 \\ D_{jv}^0 \end{Bmatrix} = \mathbf{M}_v(k_\mathrm{p}^1 a_0, k_\mathrm{sv}^1 a_0) \begin{Bmatrix} A_{jv}^1 \\ B_{jv}^1 \end{Bmatrix} + \mathbf{K}_v(k_\mathrm{p}^1 a_0, k_\mathrm{sv}^1 a_0) \begin{Bmatrix} C_{jv}^1 \\ D_{jv}^1 \end{Bmatrix}. \tag{24}$$

The conditions of continuity of stress at P_j^n, P_j^l $(l = 1, 2, \ldots, n-1)$ and P_j^0 similarly give

$$\mu_n \mathbf{L}_v(k_\mathrm{p}^n a_n, k_\mathrm{sv}^n a_n) \begin{Bmatrix} A_{jv}^n \\ B_{jv}^n \end{Bmatrix} + \mu_n \mathbf{N}_v(k_\mathrm{p}^n a_n, k_\mathrm{sv}^n a_n) \begin{Bmatrix} C_{jv}^n \\ D_{jv}^n \end{Bmatrix} = \mu \mathbf{L}_v(k_\mathrm{p} a_n, k_\mathrm{sv} a_n) \begin{Bmatrix} A_{jv} \\ B_{jv} \end{Bmatrix} + \mu \mathbf{N}_v(k_\mathrm{p} a_n, k_\mathrm{sv} a_n) \begin{Bmatrix} \Phi_v^j \\ \Psi_v^j \end{Bmatrix}, \tag{25}$$

$$\mu_l \mathbf{L}_v(k_\mathrm{p}^l a_l, k_\mathrm{sv}^l a_l) \begin{Bmatrix} A_{jv}^l \\ B_{jv}^l \end{Bmatrix} + \mu_l \mathbf{N}_v(k_\mathrm{p}^l a_l, k_\mathrm{sv}^l a_l) \begin{Bmatrix} C_{jv}^l \\ D_{jv}^l \end{Bmatrix} = \mu_{l+1} \mathbf{L}_v(k_\mathrm{p}^{l+1} a_l, k_\mathrm{sv}^{l+1} a_l) \begin{Bmatrix} A_{jv}^{l+1} \\ B_{jv}^{l+1} \end{Bmatrix} + \mu_{l+1} \mathbf{N}_v(k_\mathrm{p}^{l+1} a_l, k_\mathrm{sv}^{l+1} a_l) \begin{Bmatrix} C_{jv}^{l+1} \\ D_{jv}^{l+1} \end{Bmatrix}, \tag{26}$$

$$\mu_0 \mathbf{N}_v(k_\mathrm{p}^0 a_0, k_\mathrm{sv}^0 a_0) \begin{Bmatrix} C_{jv}^0 \\ D_{jv}^0 \end{Bmatrix} = \mu_1 \mathbf{L}_v(k_\mathrm{p}^1 a_0, k_\mathrm{sv}^1 a_0) \begin{Bmatrix} A_{jv}^1 \\ B_{jv}^1 \end{Bmatrix} + \mu_1 \mathbf{N}_v(k_\mathrm{p}^1 a_0, k_\mathrm{sv}^1 a_0) \begin{Bmatrix} C_{jv}^1 \\ D_{jv}^1 \end{Bmatrix}, \tag{27}$$

where

$$\mathbf{L}_v(k_\mathrm{p}^n a_n, k_\mathrm{sv}^n a_n) = \begin{bmatrix} L_{11}^v(k_\mathrm{p}^n a_n) & L_{12}^v(k_\mathrm{sv}^n a_n) \\ L_{21}^v(k_\mathrm{p}^n a_n) & L_{22}^v(k_\mathrm{sv}^n a_n) \end{bmatrix}, \tag{28}$$

$$\begin{cases} L_{11}^v(k_\mathrm{p}^n a_n) = \left\{ v^2 - v - \frac{(k_\mathrm{sv}^n a_n)^2}{2} \right\} H_v(k_\mathrm{p}^n a_n) + k_\mathrm{p}^n a_n H_{v+1}(k_\mathrm{p}^n a_n), \\ L_{12}^v(k_\mathrm{sv}^n a_n) = \mathrm{i}v\{(v-1) H_v(k_\mathrm{sv}^n a_n) - k_\mathrm{sv}^n a_n H_{v+1}(k_\mathrm{sv}^n a_n)\}, \\ L_{21}^v(k_\mathrm{p}^n a_n) = \mathrm{i}v\{(v-1) H_v(k_\mathrm{p}^n a_n) - k_\mathrm{p}^n a_n H_{v+1}(k_\mathrm{p}^n a_n)\}, \\ L_{22}^v(k_\mathrm{sv}^n a_n) = -\left\{ v^2 - v - \frac{(k_\mathrm{sv}^n a_n)^2}{2} \right\} H_v(k_\mathrm{sv}^n a_n) - k_\mathrm{sv}^n a_n H_{v+1}(k_\mathrm{sv}^n a_n) \end{cases} \tag{29}$$

and a similar expression for $\mathbf{N}_v(k_\mathrm{p}^n a_n, k_\mathrm{sv}^n a_n)$ with $H_v(\ )$ replaced by $J_v(\ )$ in Eqs. (28) and (29). Solving these equations interactively, we obtain equations for the determination of A_{jv} and B_{jv} as

$$\begin{Bmatrix} A_{jv} \\ B_{jv} \end{Bmatrix} = -\mathbf{Q}_v^{-1}\mathbf{P}_v \begin{Bmatrix} \Phi_v^j \\ \Psi_v^j \end{Bmatrix} = \begin{bmatrix} \frac{\pi}{4}(k_\mathrm{p}a_0)^2 \mathrm{i}P_v & \frac{\pi}{4}(k_\mathrm{sv}a_0)^2 Q_v \\ \frac{\pi}{4}(k_\mathrm{p}a_0)^2 R_v & \frac{\pi}{4}(k_\mathrm{sv}a_0)^2 \mathrm{i}S_v \end{bmatrix} \begin{Bmatrix} \Phi_v^j \\ \Psi_v^j \end{Bmatrix}. \tag{30}$$

The matrices $\mathbf{P}_v$, $\mathbf{Q}_v$ in Eq. (30) are

$$\begin{cases} \mathbf{P}_v = \mathbf{K}_v(k_\mathrm{p}a_n, k_\mathrm{sv}a_n) - \frac{\mu}{\mu_n}\mathbf{R}_v^n(\mathbf{S}_v^n)^{-1}\mathbf{N}_v(k_\mathrm{p}a_n, k_\mathrm{sv}a_n), \\ \mathbf{Q}_v = \mathbf{M}_v(k_\mathrm{p}a_n, k_\mathrm{sv}a_n) - \frac{\mu}{\mu_n}\mathbf{R}_v^n(\mathbf{S}_v^n)^{-1}\mathbf{L}_v(k_\mathrm{p}a_n, k_\mathrm{sv}a_n). \end{cases} \tag{31}$$

The recurrence formulae for $\mathbf{R}_v^n$, $\mathbf{S}_v^n$ are given by

$$\begin{cases} \mathbf{R}_v^l = \mathbf{K}_v(k_\mathrm{p}^l a_l, k_\mathrm{sv}^l a_l) - \mathbf{M}_v(k_\mathrm{p}^l a_l, k_\mathrm{sv}^l a_l)(\mathbf{Q}_v^l)^{-1}\mathbf{P}_v^l, \\ \mathbf{S}_v^l = \mathbf{N}_v(k_\mathrm{p}^l a_l, k_\mathrm{sv}^l a_l) - \mathbf{L}_v(k_\mathrm{p}^l a_l, k_\mathrm{sv}^l a_l)(\mathbf{Q}_v^l)^{-1}\mathbf{P}_v^l, \end{cases} \tag{32}$$

$$\begin{cases} \mathbf{P}_v^l = \mathbf{K}_v(k_\mathrm{p}^l a_{l-1}, k_\mathrm{sv}^l a_{l-1}) - \frac{\mu_l}{\mu_{l-1}}\mathbf{R}_v^{l-1}(\mathbf{S}_v^{l-1})^{-1}\mathbf{N}_v(k_\mathrm{p}^l a_{l-1}, k_\mathrm{sv}^l a_{l-1}), \\ \mathbf{Q}_v^l = \mathbf{M}_v(k_\mathrm{p}^l a_{l-1}, k_\mathrm{sv}^l a_{l-1}) - \frac{\mu_l}{\mu_{l-1}}\mathbf{R}_v^{l-1}(\mathbf{S}_v^{l-1})^{-1}\mathbf{L}_v(k_\mathrm{p}^l a_{l-1}, k_\mathrm{sv}^l a_{l-1}), \end{cases} \tag{33}$$

$$\begin{cases} \mathbf{R}_v^0 = \mathbf{K}_v(k_\mathrm{p}^0 a_0, k_\mathrm{sv}^0 a_0), \\ \mathbf{S}_v^0 = \mathbf{N}_v(k_\mathrm{p}^0 a_0, k_\mathrm{sv}^0 a_0). \end{cases} \tag{34}$$

It can be shown that the coefficients P_v, Q_v, R_v, S_v have the properties,

$$P_{-v} = P_v, \quad Q_v = -Q_v, \quad R_{-v} = -R_v, \quad S_{-v} = S_v \qquad (v \geqslant 0). \tag{35}$$

3. The average field for a random distribution of circular fibers

We consider the positions of the circular fibers to be random. If we denote the position vector of o_i by $\mathbf{r}_{io}$ and the probability density of the random variable $(\mathbf{r}_{1o}, \mathbf{r}_{2o}, \ldots, \mathbf{r}_{No})$ by $p(\mathbf{r}_{1o}, \mathbf{r}_{2o}, \ldots, \mathbf{r}_{No})$, then due to the indistinguishability of the circular fibers, it is symmetric in its arguments and we have (Waterman and Truell, 1961)

$$\begin{aligned} p(\mathbf{r}_{1o}, \mathbf{r}_{2o}, \ldots, \mathbf{r}_{No}) &= p(\mathbf{r}_{io})p(\mathbf{r}_{1o}, \mathbf{r}_{2o}, \ldots, ', \ldots, \mathbf{r}_{No}|\mathbf{r}_{io}) \\ &= p(\mathbf{r}_{io})p(\mathbf{r}_{jo} \mid \mathbf{r}_{io})p(\mathbf{r}_{1o}, \mathbf{r}_{2o}, \ldots, ', \ldots, ', \ldots, \mathbf{r}_{No}|\mathbf{r}_{jo}, \mathbf{r}_{io}), \\ p(\mathbf{r}_{io}) &= p(\mathbf{r}_{1o}), \quad p(\mathbf{r}_{jo}|\mathbf{r}_{io}) = p(\mathbf{r}_{2o}|\mathbf{r}_{1o}) \qquad (i \neq j), \end{aligned} \tag{36}$$

where the probabilities with the vertical bar in their argument denote the customary conditional probabilities. A prime in the first part of Eq. (36) means $\mathbf{r}_{io}$ is absent while two primes in the second part of Eq. (36) mean both $\mathbf{r}_{io}$ and $\mathbf{r}_{jo}$ are absent. For a uniform composite, the positions of a single circular fiber are equally probable within a large region S of a cross-section of the material, and hence, its distribution is uniform with density

$$\begin{aligned} p(\mathbf{r}_{io}) &= \frac{1}{S}, \quad \mathbf{r}_{io} \in S, \\ &= 0, \quad \mathbf{r}_{io} \notin S. \end{aligned} \tag{37}$$

If now o_i, well within S, is held fixed, the distribution of the circular fibers around it will be circularly symmetrical. Thus, $p(\mathbf{r}_{jo}|\mathbf{r}_{io})$ is a function of r_{ij} alone, and we can write

$$\begin{aligned} p(\mathbf{r}_{jo}|\mathbf{r}_{io}) &= \frac{1}{S}[1-g(r_{ij})], \quad \mathbf{r}_{jo} \in S, \\ &= 0, \qquad\qquad\quad \mathbf{r}_{jo} \notin S, \end{aligned} \tag{38}$$

where the pair correlation function $g(r_{ij}) \leqslant 1$ is a decreasing function of r_{ij}. The normalization condition of $p(\mathbf{r}_{jo}|\mathbf{r}_{io})$ gives, in the limit as $S \to \infty$

$$\lim_{R\to\infty} \frac{1}{R^2} \int_0^R g(r_{ij}) r_{ij}\, \mathrm{d}r_{ij} = 0. \tag{39}$$

Due to the impossibility of interpenetration of the circular fibers and their independence when they are infinitely apart, we have

$$\begin{aligned} g(r_{ij}) &= 1, \quad r_{ij} < 2a_n, \\ &= 0, \quad r_{ij} \to \infty. \end{aligned} \tag{40}$$

A function satisfying these conditions is

$$\begin{aligned} g(r_{ij}) &= 1, && r_{ij} < 2a_n, \\ &= V\, \exp(-r_{ij}/L), && r_{ij} \geqslant 2a_n, \end{aligned} \tag{41}$$

where $V\,[0 < V \leqslant \exp(2a_n/L)]$ is the coefficient and $L > 0$ is the correlation length.

We denote the conditional expectations of a statistical quantity f when either o_i or o_i and o_j together are held fixed as

$$\begin{cases} \langle f \rangle_i = \int \cdot\, .' \cdot \int f\, p(\mathbf{r}_{1o}, .\ .'., \mathbf{r}_{No}|\mathbf{r}_{io})\, \mathrm{d}\tau_1.\ .'.\mathrm{d}\tau_N, \\ \langle f \rangle_{ij} = \int .' \, .' \cdot \int f\, p(\mathbf{r}_{1o}, .'.'., \mathbf{r}_{No}|\mathbf{r}_{io}, \mathbf{r}_{jo})\, \mathrm{d}\tau_1.\ .''.\mathrm{d}\tau_N, \end{cases} \tag{42}$$

where $\mathrm{d}\tau_i$ $(i = 1, 2, \ldots, N)$ is the volume element at $\mathbf{r}_{io}$. To determine $\langle A_{iv} \rangle_i$, $\langle B_{iv} \rangle_i$ of Eq. (30), we take the conditional expectations to obtain

$$\begin{cases} \langle A_{iv} \rangle_i = \frac{\pi}{4}(k_\mathrm{p} a_0)^2 \mathrm{i} P_v \Big[i^v \Phi_0 \exp(\mathrm{i} k_\mathrm{p} r_{io} \cos\theta_{io}) + n_0 \big(1 - \frac{1}{N}\big) \sum_{m=-\infty}^{\infty} \int_{\mathbf{r}_{io}, \mathbf{r}_{jo} \in S} \{1 - g(r_{ij})\} \\ \qquad \times \langle A_{j,m+v} \rangle_{ij} H_m(k_\mathrm{p} r_{ij}) \exp(\mathrm{i} m \theta_{ji})\, \mathrm{d}\tau_j \Big] \\ + \frac{\pi}{4}(k_\mathrm{sv} a_0)^2 Q_v \Big[i^v \Psi_0 \exp(\mathrm{i} k_\mathrm{sv} r_{io} \cos\theta_{io}) + n_0 \big(1 - \frac{1}{N}\big) \sum_{m=-\infty}^{\infty} \int_{\mathbf{r}_{io}, \mathbf{r}_{jo} \in S} \{1 - g(r_{ij})\} \\ \qquad \times \langle B_{j,m+v} \rangle_{ij} H_m(k_\mathrm{sv} r_{ij}) \exp(\mathrm{i} m \theta_{ji})\, \mathrm{d}\tau_j \Big], \\ \langle B_{iv} \rangle_i = \frac{\pi}{4}(k_\mathrm{p} a_0)^2 R_v \Big[i^v \Phi_0 \exp(\mathrm{i} k_\mathrm{p} r_{io} \cos\theta_{io}) + n_0 \big(1 - \frac{1}{N}\big) \sum_{m=-\infty}^{\infty} \int_{\mathbf{r}_{io}, \mathbf{r}_{jo} \in S} \{1 - g(r_{ij})\} \\ \qquad \times \langle A_{j,m+v} \rangle_{ij} H_m(k_\mathrm{p} r_{ij}) \exp(\mathrm{i} m \theta_{ji}) \mathrm{d}\tau_j \Big] \\ + \frac{\pi}{4}(k_\mathrm{sv} a_0)^2 \mathrm{i} S_v \Big[i^v \Psi_0 \exp(\mathrm{i} k_\mathrm{sv} r_{io} \cos\theta_{io}) + n_0 \big(1 - \frac{1}{N}\big) \sum_{m=-\infty}^{\infty} \int_{\mathbf{r}_{io}, \mathbf{r}_{jo} \in S} \{1 - g(r_{ij})\} \\ \qquad \times \langle B_{j,m+v} \rangle_{ij} H_m(k_\mathrm{sv} r_{ij}) \exp(\mathrm{i} m \theta_{ji}) \mathrm{d}\tau_j \Big], \end{cases} \tag{43}$$

where $n_0 = N/S = c/\pi a_0^2$ is the number of circular fibers per unit area and c is the volume concentration of fibers in the matrix. Eq. (43) involve the conditional expectations with two circular fibers held fixed. If we take the conditional expectations of Eq. (43) with two circular fibers held fixed, the resulting equations will

contain the conditional expectations with three circular fibers held fixed, and so on. We shall eliminate this hierarchy by assuming Lax's quasicrystalline approximation (Lax, 1952), which involves the two-fiber correlation function and implies

$$\langle A_{iv}\rangle_{ij} = \langle A_{iv}\rangle_i, \quad \langle B_{iv}\rangle_{ij} = \langle B_{iv}\rangle_i, \qquad i \neq j. \tag{44}$$

According to the extinction theorem when S and N become infinitely large (Lax, 1952), the incident wave is extinguished on entering the composite, so that the corresponding terms in Eq. (43) can be dropped. Thus, these equations reduce to

$$\begin{cases} \langle A_{im}\rangle_i = \frac{ck_p^2}{4}\mathrm{i}P_m \sum_{v=-\infty}^{\infty} \int_{|\mathbf{r}_{jo}-\mathbf{r}_{io}|>2a_n} \{1-g(r_{ji})\}\langle A_{j,m+v}\rangle_j H_v(k_p r_{ji})\exp(\mathrm{i}v\theta_{ji})\,\mathrm{d}\tau_j \\ \qquad + \frac{ck_{sv}^2}{4} Q_m \sum_{v=-\infty}^{\infty} \int_{|\mathbf{r}_{jo}-\mathbf{r}_{io}|>2a_n} \{1-g(r_{ji})\}\langle B_{j,m+v}\rangle_j H_v(k_{sv} r_{ji})\exp(\mathrm{i}v\theta_{ji})\,\mathrm{d}\tau_j, \\ \langle B_{im}\rangle_i = \frac{ck_p^2}{4} R_m \sum_{v=-\infty}^{\infty} \int_{|\mathbf{r}_{jo}-\mathbf{r}_{io}|>2a_n} \{1-g(r_{ji})\}\langle A_{j,m+v}\rangle_j H_v(k_p r_{ji})\exp(\mathrm{i}v\theta_{ji})\,\mathrm{d}\tau_j \\ \qquad + \frac{ck_{sv}^2}{4}\mathrm{i}S_m \sum_{v=-\infty}^{\infty} \int_{|\mathbf{r}_{jo}-\mathbf{r}_{io}|>2a_n} \{1-g(r_{ji})\}\langle B_{j,m+v}\rangle_j H_v(k_{sv} r_{ji})\exp(\mathrm{i}v\theta_{ji})\,\mathrm{d}\tau_j. \end{cases} \tag{45}$$

Assuming the existence of the coherent wave, we try, for Eq. (45), the solutions

$$\langle A_{im}\rangle_i = i^m X_m \exp(\mathrm{i}Kx_{io}), \qquad \langle B_{im}\rangle_i = i^{m+1} Y_m \exp(\mathrm{i}Kx_{io}), \qquad x_{io} = r_{io}\cos\theta_{io}, \tag{46}$$

where X_m, Y_m are constants and K is the complex wave number of the coherent wave. The integrals not containing the pair correlation function $g(r_{ji})$ can be evaluated by using Green's theorem and the plane wave expansion. The integrals containing the pair correlation function $g(r_{ji})$ in Eq. (45) can be also simplified, and Eq. (45) reduces to the system of equations

$$\begin{cases} X_m = -cP_m \sum_{v=-\infty}^{\infty} F_v X_{m+v} - cQ_m \sum_{v=-\infty}^{\infty} G_v Y_{m+v}, \\ Y_m = cR_m \sum_{v=-\infty}^{\infty} F_v X_{m+v} - cS_m \sum_{v=-\infty}^{\infty} G_v Y_{m+v}, \end{cases} \tag{47}$$

where

$$F_v = \frac{1}{2}\mathrm{i}\pi\left[\left(\frac{a_n k_p^2}{K^2-k_p^2}\right)\left\{J_v(2Ka_n)\frac{\partial}{\partial a_n}H_v(2k_p a_n) - H_v(2k_p a_n)\frac{\partial}{\partial a_n}J_v(2Ka_n)\right\} + k_p^2\int_{2a_n}^{\infty} g(r_{ji})J_v(Kr_{ji})H_v(k_p r_{ji})r_{ji}\,\mathrm{d}r_{ji}\right] \tag{48}$$

and a similar expression for G_v with k_p replaced by k_{sv}. It is to be noted that

$$F_{-v} = F_v, \quad G_{-v} = G_v. \tag{49}$$

Eq. (47) can be combined by using Eqs. (35) and (49) to yield

$$\begin{cases} X_m + X_{-m} = -cP_m\left\{2F_m X_0 + \sum_{v=1}^{\infty}(F_{v-m}+F_{v+m})(X_v+X_{-v})\right\} - cQ_m\sum_{v=1}^{\infty}(G_{v-m}-G_{v+m})(Y_v-Y_{-v}), \\ Y_m - Y_{-m} = cR_m\left\{2F_m X_0 + \sum_{v=1}^{\infty}(F_{v-m}+F_{v+m})(X_v+X_{-v})\right\} - cS_m\sum_{v=1}^{\infty}(G_{v-m}-G_{v+m})(Y_v-Y_{-v}), \end{cases} \tag{50}$$

$$\begin{cases} X_m - X_{-m} = -cP_m \sum_{v=1}^{\infty} (F_{v-m} - F_{v+m})(X_v - X_{-v}) - cQ_m \left\{ 2G_m Y_0 + \sum_{v=1}^{\infty} (G_{v-m} + G_{v+m})(Y_v + Y_{-v}) \right\}, \\ Y_m + Y_{-m} = cR_m \sum_{v=1}^{\infty} (F_{v-m} - F_{v+m})(X_v - X_{-v}) - cS_m \left\{ 2G_m Y_0 + \sum_{v=1}^{\infty} (G_{v-m} + G_{v+m})(Y_v + Y_{-v}) \right\}, \end{cases} \tag{51}$$

where $m \geqslant 0$. If we eliminate $(X_m + X_{-m})$, $(Y_m - Y_{-m})$ from Eq. (50) and $(X_m - X_{-m})$, $(Y_m + Y_{-m})$ from Eq. (51), we obtain two equations for K in the form of infinite determinants. It can be shown that the values of K thus determined are the complex wave numbers K_{p}, K_{sv} of the coherent P and SV waves, respectively. The effects of multiple scattering on the coherent waves are of great practical importance for the concentration $c = 0.01$–0.4. At very low concentrations ($c < 0.01$), multiple scattering can be neglected and each scatterer can be treated as independent.

Assuming $k_{\mathrm{p}}a_0$, $k_{\mathrm{sv}}a_0$ and L to be sufficiently small, compared to the wave length, we obtain from Eq. (48) by expanding the Bessel and Hankel functions and retaining the lowest order terms

$$F_v \simeq \frac{1}{1 - (K/k_{\mathrm{p}})^2} \left(\frac{K}{k_{\mathrm{p}}} \right)^{|v|} + L_v, \tag{52}$$

where

$$\begin{cases} L_0 = -V \; k_{\mathrm{p}}^2 L^2 \left\{ 1 + \ln \left(\frac{1}{2} k_{\mathrm{p}} L \right) - \frac{1}{2} \mathrm{i}\pi \right\}, \\ L_v = \frac{1}{2v} V \; k_{\mathrm{p}}^2 L^2 \left(\frac{K}{k_{\mathrm{p}}} \right)^v, \quad v \geqslant 1 \end{cases} \tag{53}$$

and similar expressions for G_v, I_v with k_{p} replaced by k_{sv}. The effective in-plane bulk modulus k^* and shear modulus μ^* can be easily obtained from the phase velocities $\mathrm{Re}(k_{\mathrm{p}}/K_{\mathrm{p}})$, $\mathrm{Re}(k_{\mathrm{sv}}/K_{\mathrm{sv}})$ of the effective P and SV waves as follows:

$$k^* = \left(\frac{\rho^*}{\rho} \right) \left[(\lambda + 2\mu) \left\{ \mathrm{Re} \left(\frac{k_{\mathrm{p}}}{K_{\mathrm{p}}} \right) \right\}^2 - \mu \left\{ \mathrm{Re} \left(\frac{k_{\mathrm{sv}}}{K_{\mathrm{sv}}} \right) \right\}^2 \right], \tag{54}$$

$$\mu^* = \mu \left(\frac{\rho^*}{\rho} \right) \left\{ \mathrm{Re} \left(\frac{k_{\mathrm{sv}}}{K_{\mathrm{sv}}} \right) \right\}^2, \tag{55}$$

where the average mass density ρ^* is

$$\rho^* = \rho \left\{ 1 - c \left(1 + \frac{h}{a_0} \right)^2 \right\} + \rho_0 c + \sum_{l=1}^{n} \rho_l c \left\{ \frac{1}{n} \frac{h}{a_0} \left(2 + \frac{2l-1}{n} \frac{h}{a_0} \right) \right\}. \tag{56}$$

4. Numerical results and discussions

To examine the effect of interface properties on the phase velocities and attenuations of coherent plane waves through the composite medium, for a given value of $k_{\mathrm{sv}}a_0 = a_0\omega/c_{\mathrm{sv}}$, the coefficients P_v, Q_v, R_v, S_v are computed. Next, the complex coefficient matrix M (or N) corresponding to $(X_m + X_{-m})$, $(Y_m - Y_{-m})$ (Eq. (50)) (or $(X_m - X_{-m})$, $(Y_m + Y_{-m})$ (Eq. (51)) is formed. The complex determinant of the coefficient matrix is computed using standard Gauss elimination techniques. For a given $a_0\omega/c_{\mathrm{sv}}$, the root of the equation $\det M = 0$ (or $\det N = 0$) is searched in the complex K_{p} (or K_{sv}) plane using Muller's method. The efficacy of the quasicrystalline approximation depends on the accuracy of the spatial correlation between two fibers, i.e., the pair correlation function (Kim, 1996). For the statistical parameters, we take $V = \exp(2a_n/L) \approx 1$

Table 1
Material properties of SiC and Al

SiC	ρ_0 (kg/m^3)	μ_0 (GPa)	$\lambda_0 + 2\mu_0$ (GPa)	v_0
	3181	188.1	474.2	0.17
Al	ρ (kg/m^3)	μ (GPa)	$\lambda + 2\mu$ (GPa)	v
	2706	26.7	110.5	0.34

and tentatively take $L = L_0 c$. Good initial guesses are provided by Eq. (50) (or Eq. (51)) and Eqs. (52) and (53) at low values of $a_0\omega/c_{sv}$ and these can be used systematically to obtain quick convergence of roots at increasingly higher values of $a_0\omega/c_{sv}$. The values of K_p and K_{sv}, as determined above, are obviously complex. For the relevant roots, the real and imaginary parts should be positive. The phase velocities of propagation of the coherent P and SV waves are $\mathrm{Re}(k_p/K_p)$ and $\mathrm{Re}(k_{sv}/K_{sv})$, respectively. Their corresponding attenuations are $\mathrm{Im}(K_p/k_p)$ and $\mathrm{Im}(K_{sv}/k_{sv})$. The considered composite was a SiC–Al composite. The constituent properties are given in Table 1.

One of the used environments for most of the metal matrix composite systems is the thermal environment, particularly in high temperatures. It is to be noted that minimization of overall thermal stresses in a composite medium is desirable for better structural reliability in the actual application. The common problem has been the large difference in thermal expansion characteristics of ceramics and metals (Taya and Arsenault, 1989). A typical functionally graded material (FGM) structure consists of a change from fully ceramic on one side to fully metal on the other side, with the intermediate regions consisting of a mixture of both constituents, varying in volume concentration with distance. Such a design would allow a gradual change in thermal expansion mismatch, minimizing the thermal stresses arising from cooling or heating. Controlled deposition of two materials is feasible in techniques such as chemical vapor deposition (CVD) method (Uemura et al., 1990).

First of all, we consider a graded interface layer which consists of varying proportions of SiC and Al. Two special cases of graded interface material are considered. The volume concentrations c_q $(q = \mathrm{I}, \mathrm{II})$ of SiC for Cases I and II are given by

Case I

$$c_{\mathrm{I}}(r_i) = \begin{cases} 1 & (r_i \leqslant a_0), \\ \frac{1}{2} & (a_0 \leqslant r_i \leqslant a_0 + h), \\ 0 & (a_0 + h \leqslant r_i), \end{cases} \tag{57}$$

Case II

$$c_{\mathrm{II}}(r_i) = \begin{cases} 1 & (r_i \leqslant a_0), \\ \left(1 - \frac{r_i - a_0}{h}\right)^{\gamma} & (a_0 \leqslant r_i \leqslant a_0 + h), \\ 0 & (a_0 + h \leqslant r_i). \end{cases} \tag{58}$$

Using these equations, a number of profiles in the variation of volume concentration of SiC with distance can be examined, by varying the exponent γ. The variations in volume concentrations of SiC along the radial axis are shown in Fig. 2 for Cases I and II. Due to the changes in relative proportions of SiC and Al, elastic properties vary across the thickness of the graded interface layer. The Lamé constants λ_q and μ_q of the graded interface layer are considered to vary as (Tuchinskii, 1983)

$$\lambda_q(r_i) = \frac{E_q v_q}{(1 + v_q)(1 - 2v_q)} \quad (q = \mathrm{I}, \mathrm{II},\ a_0 \leqslant r_i \leqslant a_0 + h), \tag{59}$$

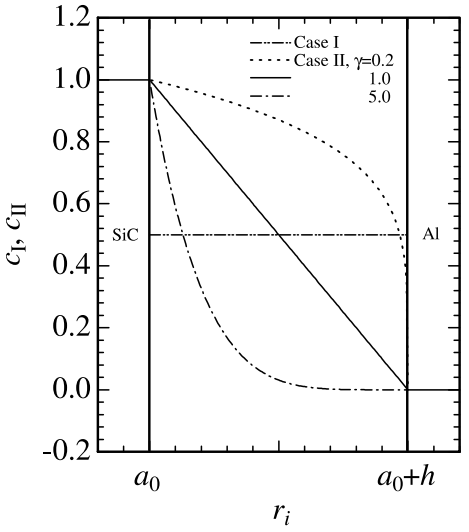

Fig. 2. The forms of variations in the volume concentration of SiC in a graded interface layer.

$$\mu_q(r_i) = \frac{E_q}{2(1+\nu_q)} \quad (q = \mathrm{I}, \mathrm{II},\ a_0 \leqslant r_i \leqslant a_0 + h), \tag{60}$$

where E_q and ν_q are the Young's modulus and the Poisson's ratio of the graded interface layer in the form

$$E_q(r_i) = 2\left[\frac{1-c_q}{\mu(1+\nu)(1-c_q^2)+\mu_0(1+\nu_0)c_q^2} + \frac{c_q}{\mu(1+\nu)(1-c_q)^2+\mu_0(1+\nu_0)(2-c_q)c_q}\right]^{-1}, \tag{61}$$

$$\nu_q(r_i) = \frac{\{\nu - c_q^2(\nu-\nu_0 c_q^2)\}\{1-c_q(1-\alpha)\}}{\{1-c_q(1-\beta)\}\{1-c_q(1-1/\beta)\}} \tag{62}$$

with

$$\alpha = \frac{\nu(1-c_q)^2 + \nu_0(2-c_q)c_q}{\nu(1-c_q^2)+\nu_0 c_q^2}, \tag{63}$$

$$\beta = \frac{\mu(1+\nu)(1-c_q)^2 + \mu_0(1+\nu_0)(2-c_q)c_q}{\mu(1+\nu)(1-c_q^2)+\mu_0(1+\nu_0)c_q^2}. \tag{64}$$

The density is given by

$$\rho_q(r_i) = \rho(1-c_q) + \rho_0 c_q \quad (q = \mathrm{I}, \mathrm{II},\ a_0 \leqslant r_i \leqslant a_0 + h). \tag{65}$$

The material properties of the layers given above are calculated at the midpoint of each layer assuming variations of Cases I and II from the boundary of the fiber to the matrix medium. Among the functional forms considered, the linear variation of Case II ($\gamma = 1.0$) in composition, across the graded interface layer, will result in the least residual stresses in all types of structures.

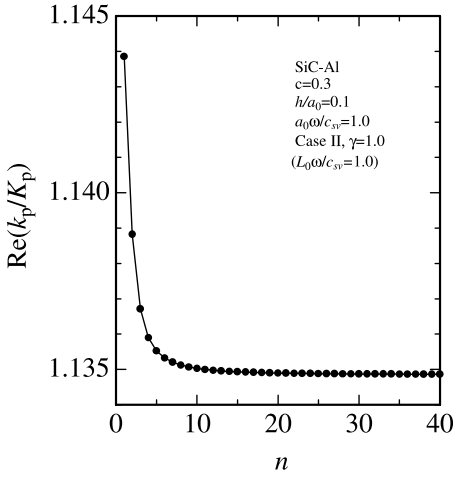

Fig. 3. Phase velocity vs n for P wave scattering.

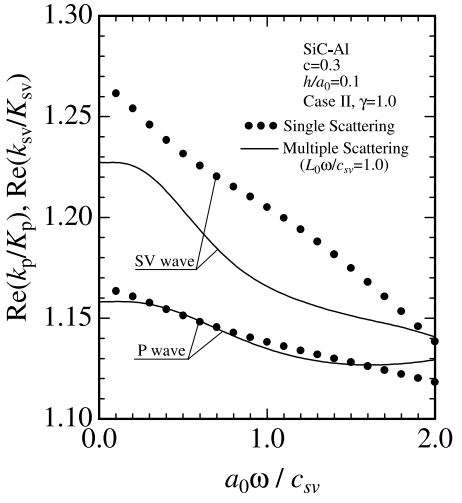

Fig. 4. Effect of multiple scattering on phase velocities vs frequency for effective P and SV waves.

Fig. 3 shows the variation of the phase velocity $\mathrm{Re}(k_p/K_p)$ of the effective P wave with the number of layers n for Case II ($\gamma = 1.0$) and $c = 0.3$, $h/a_0 = 0.1$, $a_0\omega/c_{sv} = 1.0$ ($k_{sv}L_0 = L_0\omega/c_{sv} = 1.0$). Case II ($\gamma = 1.0$) refers to the case of the interface material through which the volume concentration varies linearly from that of the fibers to that of the matrix. It is found that the truncation after $n = 30$ gives practically adequate results for Case II ($\gamma = 1.0$). In Fig. 4, we have shown a comparison of the results of multiple scattering ($L_0\omega/c_{sv} = 1.0$) with the results of single scattering, where we had studied the phase velocities $\mathrm{Re}(k_p/K_p)$, $\mathrm{Re}(k_{sv}/K_{sv})$ of the effective P and SV waves with the frequency $a_0\omega/c_{sv}$ for Case II ($\gamma = 1.0$) and $c = 0.3$, $h/a_0 = 0.1$. One sees from the figure that the discrepancies in the phase velocities obtained by these two methods appear for the frequency considered. The effect of the graded interface layer on $\mathrm{Re}(k_p/K_p)$ at $a_0\omega/c_{sv} = 1.0$ for Case I, Case II ($\gamma = 0.2, 1.0, 5.0$) and $c = 0.3$ ($L_0\omega/c_{sv} = 1.0$) is shown in Fig. 5. The figure shows that the phase velocity $\mathrm{Re}(k_p/K_p)$ increases with the h/a_0 ratio, and depends on the

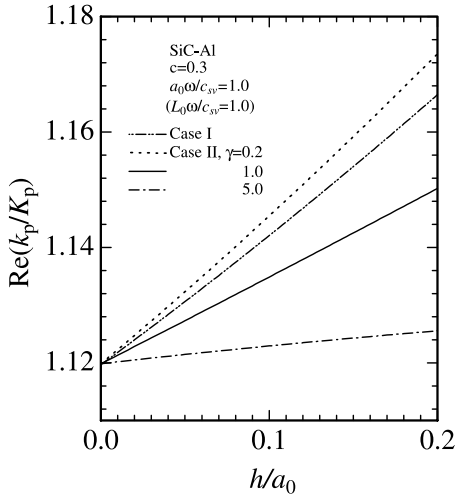

Fig. 5. Phase velocities vs h/a_0 for P wave scattering.

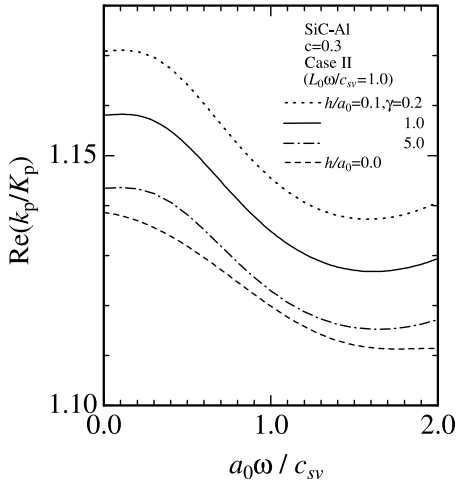

Fig. 6. Effect of graded interface layer on phase velocity vs frequency for P wave.

constituents and the nature of the interface layer. The phase velocity for Case II, which was evaluated by taking $n = 30$ and 32, agreed to at least three decimal places. Thus, it may be said that the result for $n = 30$ is, from a practical view point, quite satisfactory.

Figs. 6 and 7 show the variations of the phase velocities $\mathrm{Re}(k_\mathrm{p}/K_\mathrm{p})$, $\mathrm{Re}(k_\mathrm{sv}/K_\mathrm{sv})$ of the effective P and SV waves with the frequency $a_0\omega/c_\mathrm{sv}$ for Case II ($\gamma = 0.2, 1.0, 5.0$) and $c = 0.3$, $h/a_0 = 0.0, 0.1$ ($L_0\omega/c_\mathrm{sv} = 1.0$). The interface effect increases the phase velocities. Figs. 8 and 9 show the variations of the attenuations $\mathrm{Im}(K_\mathrm{p}/k_\mathrm{p})$, $\mathrm{Im}(K_\mathrm{sv}/k_\mathrm{sv})$ of the effective P and SV waves with the frequency $a_0\omega/c_\mathrm{sv}$ for Case II ($\gamma = 0.2, 1.0, 5.0$) and $c = 0.3$, $h/a_0 = 0.0, 0.1$ ($L_0\omega/c_\mathrm{sv} = 1.0$). The attenuations increase with the frequency. The computations carried out reveal that the truncation after $n = 30$ gives practically adequate results at any desired finite frequency for Case II.

Fig. 10 shows the variation of the effective in-plane bulk modulus k^* of SiC–Al with the frequency $a_0\omega/c_\mathrm{sv}$ for Case II ($\gamma = 0.2, 1.0, 5.0$) and $c = 0.3$, $h/a_0 = 0.0, 0.1$ ($L_0\omega/c_\mathrm{sv} = 1.0$). The interface effect in-

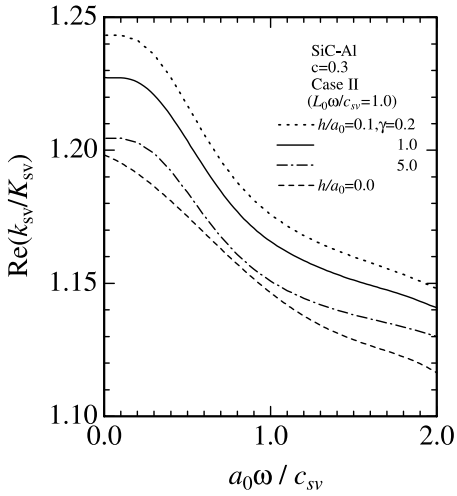

Fig. 7. Effect of graded interface layer on phase velocity vs frequency for SV wave.

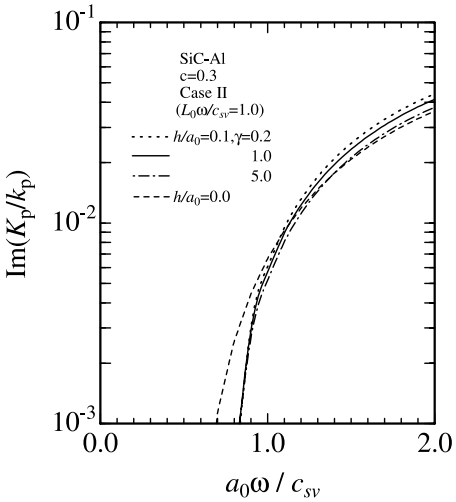

Fig. 8. Effect of graded interface layer on attenuation vs frequency for P wave.

creases the effective in-plane bulk modulus. Fig. 11 also shows the variation of the effective in-plane shear modulus μ^* of SiC–Al with the frequency $a_0\omega/c_{sv}$ for Case II ($\gamma = 0.2, 1.0, 5.0$) and $c = 0.3$, $h/a_0 = 0.0, 0.1$ ($L_0\omega/c_{sv} = 1.0$). The effective in-plane shear modulus decreases as the frequency increases and the interface effect increases the effective in-plane shear modulus.

Secondly, we consider an imperfect interface layer. When the interface layer includes different microdefects such as porosity, inclusions, or cracks, the elastic moduli are smaller than those of the fiber (Huang et al., 1997). Four special cases of imperfect interface material are considered. The elastic properties of Cases III a–d are given by

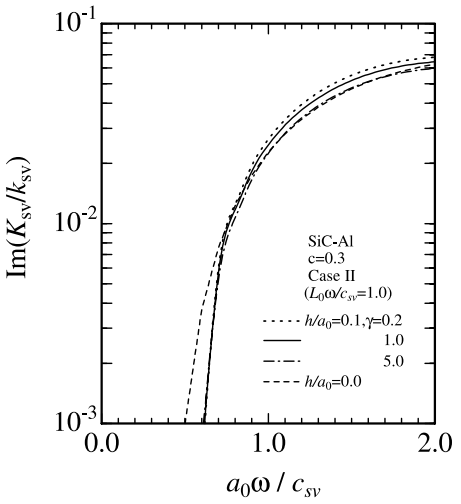

Fig. 9. Effect of graded interface layer on attenuation vs frequency for SV wave.

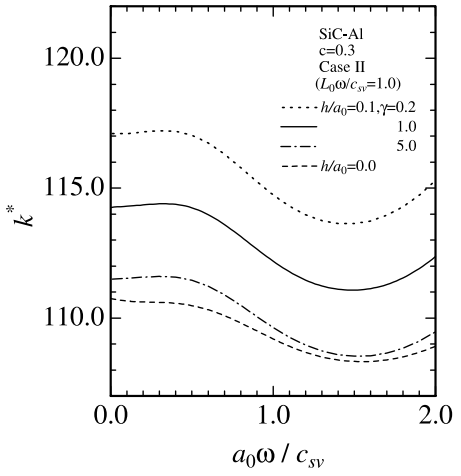

Fig. 10. Effect of graded interface layer on effective in-plane bulk modulus vs frequency.

Case III a

$$\begin{aligned}\lambda_{\mathrm{III}}(r_i) &= \lambda_0,\\ \mu_{\mathrm{III}}(r_i) &= \mu_0,\\ \rho_{\mathrm{III}}(r_i) &= \rho_0 \quad (a_0 \leqslant r_i \leqslant a_0 + h),\end{aligned} \tag{66}$$

Case III b

$$\begin{aligned}\lambda_{\mathrm{III}}(r_i) &= \frac{\lambda + \lambda_0}{2},\\ \mu_{\mathrm{III}}(r_i) &= \frac{\mu + \mu_0}{2},\\ \rho_{\mathrm{III}}(r_i) &= \frac{\rho + \rho_0}{2} \quad (a_0 \leqslant r_i \leqslant a_0 + h),\end{aligned} \tag{67}$$

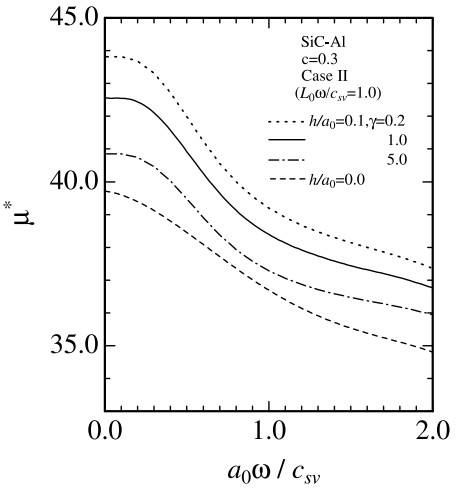

Fig. 11. Effect of graded interface layer on effective in-plane shear modulus vs frequency.

Case III c

$$\begin{aligned}\lambda_{\mathrm{III}}(r_i) &= \lambda,\\ \mu_{\mathrm{III}}(r_i) &= \mu,\\ \rho_{\mathrm{III}}(r_i) &= \rho \quad (a_0 \leqslant r_i \leqslant a_0 + h),\end{aligned} \tag{68}$$

Case III d

$$\begin{aligned}\lambda_{\mathrm{III}}(r_i) &= \lambda - \frac{\lambda_0 - \lambda}{10},\\ \mu_{\mathrm{III}}(r_i) &= \mu - \frac{\mu_0 - \mu}{10},\\ \rho_{\mathrm{III}}(r_i) &= \rho - \frac{\rho_0 - \rho}{10} \quad (a_0 \leqslant r_i \leqslant a_0 + h).\end{aligned} \tag{69}$$

Figs. 12 and 13 show the variations of the phase velocities $\mathrm{Re}(k_{\mathrm{p}}/K_{\mathrm{p}})$, $\mathrm{Re}(k_{\mathrm{sv}}/K_{\mathrm{sv}})$ of the effective P and SV waves with the frequency $a_0\omega/c_{\mathrm{sv}}$ for Cases III a–d and $c = 0.3$, $h/a_0 = 0.1$ ($L_0\omega/c_{\mathrm{sv}} = 1.0$). Figs. 14 and 15 show the variations of the attenuations $\mathrm{Im}(K_{\mathrm{p}}/k_{\mathrm{p}})$, $\mathrm{Im}(K_{\mathrm{sv}}/k_{\mathrm{sv}})$ of the effective P and SV waves with the frequency $a_0\omega/c_{\mathrm{sv}}$ for Cases III a–d and $c = 0.3$, $h/a_0 = 0.1$ ($L_0\omega/c_{\mathrm{sv}} = 1.0$).

Finally, we consider the static effective elastic constants of composites. As $a_0\omega/c_{\mathrm{sv}} \to 0$, the dynamic effective in-plane bulk modulus and shear modulus tend to the static solutions. The expressions for the static effective elastic constants of composites are given in Appendix A. Fig. 16 shows the variation of the static effective in-plane bulk modulus k^* with the volume concentration c for $h/a_0 = 0.0$. A comparison of the static effective in-plane bulk modulus is made in $a_0\omega/c_{\mathrm{sv}} = 0.0$ ($L_0\omega/c_{\mathrm{sv}} = 0.01$), Eshelby method (Eq. (A.1)), law of mixture (Eq. (A.3)) and the composite cylinder assemblage (CCA) model (Hashin and Rosen, 1964) (Eq. (A.5)). It should be emphasized that the results agree much better with those obtained from the Eshelby method and the CCA model over the full range of the concentration. In Fig. 17, the static effective in-plane shear modulus μ^* is plotted as a function of concentration c for $a_0\omega/c_{\mathrm{sv}} = 0.0$, $h/a_0 = 0.0$ ($L_0\omega/c_{\mathrm{sv}} = 0.01$) and also compared with Eshelby method (Eq. (A.2)), law of mixture (Eq. (A.4)) and the generalized self consistent model (GSCM) (Christensen and Lo, 1979) (Eq. (A.6)). Again, the agreement in

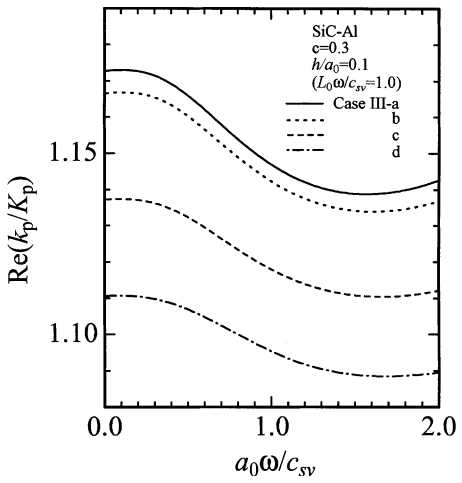

Fig. 12. Effect of imperfect interface layer on phase velocity vs frequency for P wave.

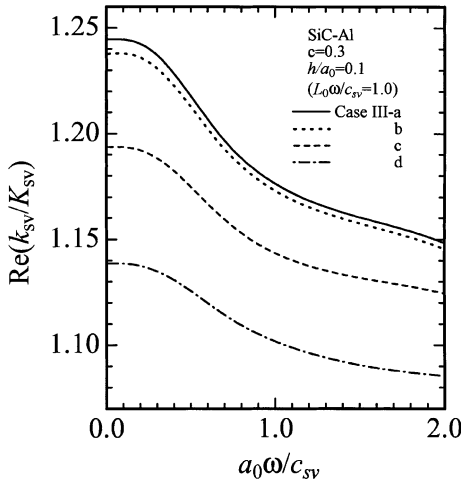

Fig. 13. Effect of imperfect interface layer on phase velocity vs frequency for SV wave.

the static effective in-plane shear modulus calculated from the present theory and from the Eshelby method is excellent.

In conclusion, the multiple scattering of compressional and shear waves by circular fibers with thick nonhomogeneous interface layers was analyzed. The interface effect can vary phase velocities, attenuations of coherent plane waves in a metal matrix composite and effective elastic constants, and depends on the frequency and the material properties of the interface layers. The numerical results at the volume concentration of fibers, $c = 0.3$, were obtained for any given finite frequency, and layers with nonhomogeneous elastic properties of any desired finite thickness. Specially designed interface layers are used in modern composites to improve fracture toughness, chemical compatibility, and matching of thermal expansion

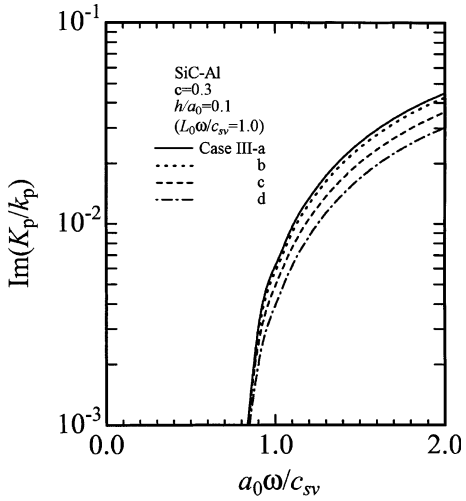

Fig. 14. Effect of imperfect interface layer on attenuation vs frequency for P wave.

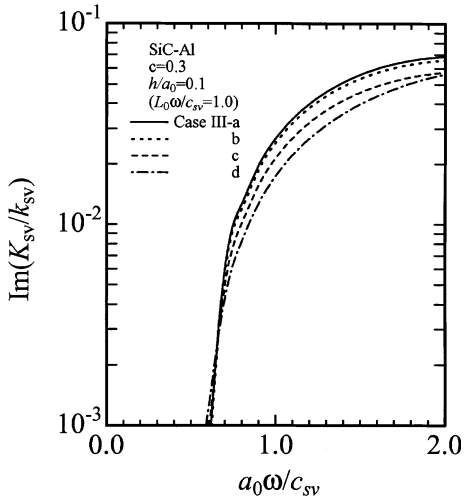

Fig. 15. Effect of imperfect interface layer on attenuation vs frequency for SV wave.

coefficients between composite constituents. It is hoped that this study will help in assessing the feasibility of determining interface characteristics by ultrasonic means.

Appendix A

Using the Eshelby method, we obtain the effective in-plane bulk modulus k^* and shear modulus μ^* as Wakashima (1976).

$$k^* = (1-c)k + ck_0 + c(1-c)\frac{(k_0-k)(1/k_0-1/k)}{(1-c)/k + c/k_0 + \mu/kk_0}, \tag{A.1}$$

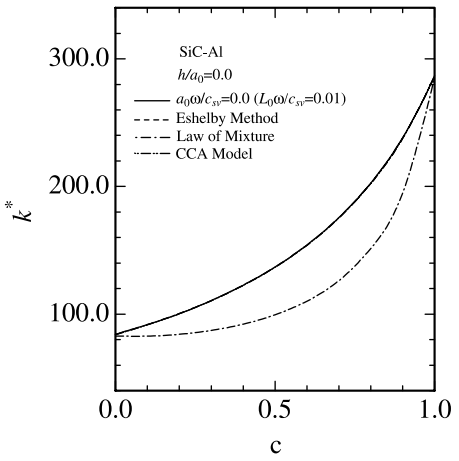

Fig. 16. Static effective in-plane bulk modulus vs concentration.

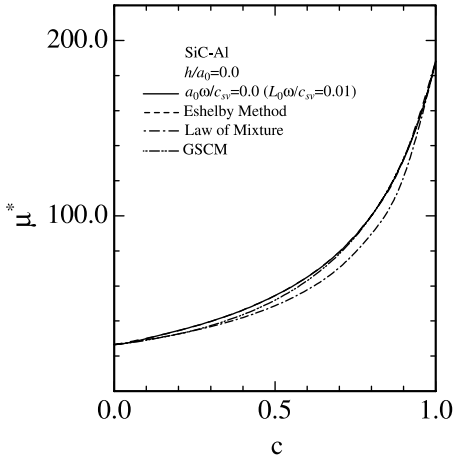

Fig. 17. Static effective in-plane shear modulus vs concentration.

$$\mu^* = (1-c)\mu + c\mu_0 + c(1-c)\frac{(\mu_0-\mu)(1/\mu_0 - 1/\mu)}{(1-c)/\mu + c/\mu_0 + (k/\mu_0)/(k+2\mu)}, \tag{A.2}$$

where $k = \lambda + \mu$, $k_0 = \lambda_0 + \mu_0$ are the in-plane bulk moduli of the matrix and fiber. Making use of the law of mixture, we also have

$$k^* = \frac{E^*}{2(1+\nu^*)(1-2\nu^*)}, \tag{A.3}$$

$$\mu^* = \frac{E^*}{2(1+\nu^*)}, \tag{A.4}$$

where E^* and v^* are the Young's modulus and Poisson's ratio of a fiber-reinforced composite in the form

$$E^* = \frac{2(1+v_0)(1+v)\mu_0\mu}{(1+v_0)\mu_0(1-c)+(1+v)\mu c},$$

$$v^* = v(1-c)+v_0 c.$$

Using the CCA model (Hashin and Rosen, 1964), we also obtain the effective in-plane bulk modulus k^* of a fiber-reinforced composite in the form

$$k^* = k + \frac{c(k_0-k)(k+\mu)}{k_0+\mu-c(k_0-\mu)}. \tag{A.5}$$

The GSCM (Christensen and Lo, 1979) yields an expression for the effective in-plane shear modulus over the entire volume fraction range. Their result is the quadratic equation

$$A\left(\frac{\mu^*}{\mu}\right) + 2B\left(\frac{\mu^*}{\mu}\right) + C = 0, \tag{A.6}$$

where

$$\begin{aligned}
A &= 3c(1-c)^2\left(\frac{\mu_0}{\mu}-1\right)\left(\frac{\mu_0}{\mu}+\eta_0\right) + \left\{\frac{\mu_0}{\mu}\eta+\eta_0\eta-\left(\frac{\mu_0}{\mu}\eta-\eta_0\right)c^3\right\}\left\{\eta c\left(\frac{\mu_0}{\mu}-1\right)-\left(\frac{\mu_0}{\mu}\eta+1\right)\right\},\\
B &= -3c(1-c)^2\left(\frac{\mu_0}{\mu}-1\right)\left(\frac{\mu_0}{\mu}+\eta_0\right)\\
&\quad+\frac{1}{2}\left\{\frac{\mu_0}{\mu}\eta+\left(\frac{\mu_0}{\mu}-1\right)c+1\right\}\left\{\left(\frac{\mu_0}{\mu}-1\right)\left(\frac{\mu_0}{\mu}+\eta_0\right)-2\left(\frac{\mu_0}{\mu}\eta-\eta_0\right)c^3\right\}\\
&\quad+\frac{c}{2}(\eta+1)\left(\frac{\mu_0}{\mu}-1\right)\left\{\frac{\mu_0}{\mu}+\eta_0+\left(\frac{\mu_0}{\mu}\eta-\eta_0\right)c^3\right\},\\
C &= 3c(1-c)^2\left(\frac{\mu_0}{\mu}-1\right)\left(\frac{\mu_0}{\mu}+\eta_0\right)+\left\{\frac{\mu_0}{\mu}\eta+\left(\frac{\mu_0}{\mu}-1\right)c+1\right\}\left\{\frac{\mu_0}{\mu}+\eta_0+\left(\frac{\mu_0}{\mu}\eta-\eta_0\right)c^3\right\},\\
\eta &= 3-4v,\\
\eta_0 &= 3-4v_0.
\end{aligned}$$

Appendix B

Yang and Mal (1995, 1996) have used a homogenization technique which combines the GSCM and a statistical averaging procedure to study the influence of the interface on the static and dynamic properties of composites. The material used for computations is a titanium aluminide matrix composite reinforced with coated silicon carbide fibers. The fiber volume concentration of the composite is 0.35. The constituent properties given in Table 2 are taken from Yang and Mal (1996). We have shown the results calculated from the present theory for the SiC–C–Ti composite. Fig. 18 shows the variation of the phase velocity $\mathrm{Re}(k_\mathrm{p}/K_\mathrm{p})$ of the effective P wave with the frequency $a_0\omega/c_\mathrm{sv}$ for $h/a_0 = 0.0, 0.05, 0.1$ and $c = 0.35$ $(L_0\omega/c_\mathrm{sv} = 1.0)$. The general behavior of the phase velocity is similar to that derived by Yang and Mal (1995, 1996).

Table 2
Material properties of SiC, C and Ti

SiC	ρ_0 (kg/m^3)	μ_0 (GPa)	$\lambda_0 + 2\mu_0$ (GPa)	v_0
	3200	172.0	518.8	0.25
C	ρ_1 (kg/m^3)	μ_1 (GPa)	$\lambda_1 + 2\mu_1$ (GPa)	v_1
	1400	14.3	38.6	0.21
Ti	ρ (kg/m^3)	μ (GPa)	$\lambda + 2\mu$ (GPa)	v
	4500	37.1	129.9	0.30

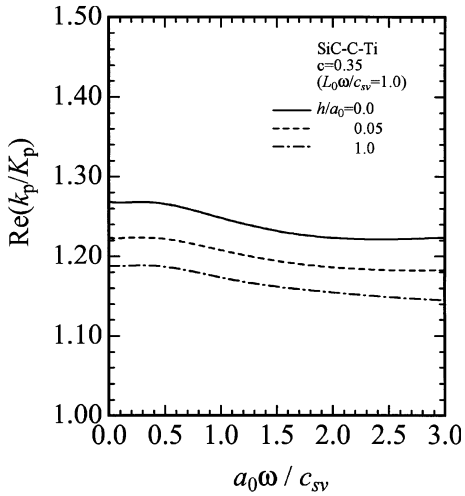

Fig. 18. Effect of interface thickness of C on phase velocity vs frequency for P wave in a SiC–C–Ti composite.

References

Bose, S.K., Mal, A.K., 1974. Elastic waves in a fiber-reinforced composite. Journal of Mechanics and Physics of Solids 22, 217–229.
Christensen, R.M., Lo, K.H., 1979. Solutions for effective shear properties in three phase sphere and cylinder models. Journal of Mechanics and Physics of Solids 27 (4), 315–330.
Hashin, Z., Rosen, R.W., 1964. The elastic moduli of fiber-reinforced materials. ASME Journal of Applied Mechanics 31 (2), 223–232.
Huang, W., Rokhlin, S.I., Wang, Y.J., 1997. Analysis of different boundary condition models for study of wave scattering from fiber-matrix interphases. Journal of the Acoustical Society of America 101 (4), 2031–2042.
Kim, J.Y., 1996. Dynamic self-consistent analysis for elastic wave propagation in fiber reinforced composites. Journal of the Acoustical Society of America 100 (4), 2002–2010.
Lax, M., 1952. Multiple scattering of waves. II. The effective field in dense systems. Physical Review 85, 621–629.
Nozaki, H., Shindo, Y., 1998. Effect of interface layers on elastic wave propagation in a fiber-reinforced metal-matrix composite. International Journal of Engineering Science 36 (4), 383–394.
Shindo, Y., Nozaki, H., Datta, S.K., 1995. Effect of interface layers on elastic wave propagation in a metal matrix composite reinforced by particles. ASME Journal of Applied Mechanics 62 (1), 178–185.
Shindo, Y., Niwa, N., 1996. Scattering of antiplane shear waves in a fiber-reinforced composite medium with interfacial layers. Acta Mechanica 117, 181–190.
Shindo, Y., Niwa, N., Togawa, R., 1998. Multiple scattering of antiplane shear waves in a fiber-reinforced composite medium with interfacial layers. International Journal of Solids and Structures 35 (7–8), 733–745.
Taya, M., Arsenault, R.J., 1989. Metal Matrix Composites, First ed. Pergamon Press, New York.

Tuchinskii, L.I., 1983. Elastic constants of pseudoalloys with a skeletal structure. Poroshkovaya Metallurgiya 247 (7), 85–92.
Uemura, S., Sohda, Y., Kude, Y., Hirai, T., Sasaki, M., 1990. Preparation and evaluation of SiC/C functionally gradient materials by chemical vapor deposition. Journal of the Japan Society of Powder and Powder Metallurgy 37 (2), 275–282 (in Japanese).
Wakashima, K., 1976. Macroscopic mechanical properties of composite materials. II. Elastic moduli and thermal expansion coefficients. Japan Society of Composite Materials 2 (4), 161–167 (in Japanese).
Waterman, P.C., Truell, R., 1961. Multiple scattering of waves. Journal of Mathematical Physics 2 (4), 512–537.
Watson, G.N., 1966. A Treatise on the Theory of Bessel Functions, Second ed. Cambridge University Press, Cambridge.
Yang, R.B., Mal, A.K., 1995. The effective transverse moduli of a composite with degraded fiber-matrix interfaces. International Journal of Engineering Science 33 (11), 1623–1632.
Yang, R.B., Mal, A.K., 1996. Elastic waves in a composite containing inhomogeneous fibers. International Journal of Engineering Science 34 (1), 67–79.